JOURNAL OF Applied Polymer SCIENCE

Performance Improvement of Piezoelectric-Rubber by Particle Formation of Linear Aggregates

Shogo Mamada,[1] Naoyuki Yaguchi,[1] Masanori Hansaka,[1] Masafumi Yamato,[2] Hirohisa Yoshida[2]

[1]Materials Technology Division, Railway Technical Research Institute, Kokubunji, Tokyo 185-8540, Japan

[2]Division of Applied Chemistry, Graduate School of Urban Environmental Science, Tokyo Metropolitan University Hachioji, Tokyo 192-0397, Japan

Correspondence to: S. Mamada (E-mail: mamada@rtri.or.jp)

ABSTRACT: We investigate the piezoelectric response of piezoelectric-rubber consisting of lead zirconate titanate (PZT) particles and silicon rubber prepared by holding it at 100°C for 60 min. Two types of piezoelectric-rubber were used; one was mixed with PZT particles forming linear aggregates, and the other was mixed with PZT particles forming a random dispersion. The piezoelectric-rubber whose PZT particles were aligned normal to the rubber surface had much higher piezoelectric effect than the type of piezoelectric-rubber whose PZT particles were randomly dispersed. The reason for this is that force applied on the former is directly transmitted to PZT particles and the electric charges generated from PZT particles had higher mobility because of the aligned PZT particles, which were connected with each other. As a result, the formation of linear aggregates of PZT particles in rubber was effective in enhancing piezoelectric properties of piezoelectric-rubber. © 2013 Wiley Periodicals, Inc. J. Appl. Polym. Sci. **2014**, *131*, 39862.

KEYWORDS: composites; elastomers; thermosets; self-assembly; sensors and actuators

Received 5 June 2013; accepted 15 August 2013

DOI: 10.1002/app.39862

INTRODUCTION

Piezoelectric materials, which have properties of converting a part of mechanical energy to electric energy and vice versa, are used as sensors and actuators. Recently, attention has been paid to them for their use as a vibration and noise reduction device and an energy conversion device.[1–7] However, the piezoelectric-ceramic which is used as standard piezoelectric material has the following problems. First, it cannot be used at places where impact and vibrating force are applied on the materials, because the materials are brittle and susceptible to damage under such force. Second, it is difficult to form it into complicated shapes. Therefore, flexible piezoelectric materials have been developed.[8–12]

As the above materials, we focused on piezoelectric-rubber which is relatively easy to fabricate. Piezoelectric-rubber, which is fabricated by polarizing under high voltage after mixing rubber with the piezoelectric-ceramic particles, is expected as the materials, which have flexibility and can be formed into arbitrary shapes.[13–21] To enhance piezoelectric properties, plenty of piezoelectric-ceramic particles need to be mixed into rubber. However, the amount of piezoelectric-ceramic particles mixed into rubber is limited to keep the character of rubber.

Therefore, a method of enhancing piezoelectric properties of piezoelectric-rubber with fewer piezoelectric-ceramic particles is required. A method in which piezoelectric-ceramic particles are aligned in rubber by means of an electric field was investigated. This method has been introduced by referring to the study of ER (electrorheological) fluid.[22–27] It is expected that the piezoelectric properties of piezoelectric-rubber will be improved by the formation of linear aggregates of piezoelectric-ceramic particles just like in the case of ER fluid. Because force applied on piezoelectric-rubber will be directly transmitted to piezoelectric-ceramic particles and the electric charge generated from piezoelectric-ceramic particles is easy to conduct though the piezoelectric-ceramic particles, which are connected with each other.

In this investigation, the influence of particle formation of linear aggregates on piezoelectric properties was investigated. Further, the influence of major material characteristics such as the concentration and size of the piezoelectric-ceramic particles on piezoelectric properties were discussed.

EXPERIMENTAL

Materials

The rubber properties required for fabricating the piezoelectric-rubber in which piezoelectric-ceramic particles form linear aggregates are, low viscosity, post curing after poling, and electrical insulation. After some trials for several materials, we selected thermosetting silicone rubber KE-106 supplied by Shin-Etsu Chemical whose properties are shown in Table I.

Table I. Properties of Silicone Rubber KE-106

Viscosity (Pa s^{-1})	Electric breakdown strength (kV mm^{-1})	Thermosetting condition (min °C)
3.5	23	30/150

Lead zirconate titanate (PZT) particle was selected as a piezoelectric-ceramic particle because it was easy to obtain and had good piezoelectric properties. In this investigation, two types of PZT named as $PZT_{DPZ\text{-}LQ\text{-}S1}$ supplied by DAINIPPONTORYO and $PZT_{Z\text{-}711}$ supplied by CERATEC Engineering was used. Both PZT were bought in particles. The properties of each PZT are shown in Table II. The piezoelectric strain constant d_{33} shown in Table II is one of the indexes of piezoelectric properties of the piezoelectric materials. It is the value of electric charge per unit of force applied on piezoelectric materials. The suffix of 33 indicates that the direction of the input force and that of output electric charge are consistent with the thickness direction of piezoelectric materials in case the vertical direction is 3.

$PZT_{DPZ\text{-}LQ\text{-}S1}$ with four different particle sizes noted as A, B, C, and D were used to examine the influence of the particle size on piezoelectric properties. Figure 1 shows the measurement result of particle size distribution of four particles by a laser diffraction particle size analyzer. The sizes of each $PZT_{DPZ\text{-}LQ\text{-}S1}$ particle were ~0.5 μm (A), 10 μm (B), 35 μm (C), and 66 μm (D), respectively. However, particle size of $PZT_{Z\text{-}711}$ was ~500 μm. With respect to particles of C of $PZT_{DPZ\text{-}LQ\text{-}S1}$ and $PZT_{Z\text{-}711}$, the concentration of PZT particles were set at 10–60 vol % to examine the influence of concentration of the particles on piezoelectric properties of piezoelectric-rubber.

Fabrication Process of the Sample

Fabrication process of the sample was as follows.

1. After PZT particles were added in uncured silicone rubber, the rubber was stirred and degassed for 3 min by a mixer.
2. The uncured silicone rubber mixed with PZT particles were poured into the space as shown Figure 2. The space was a 50 mm diameter hole prepared at the center of 2 mm thick Bakelite plate, which was placed on the grounding electrode.
3. The (+) electrode was placed on the Bakelite plate as shown in Figure 2.
4. A case containing the sample was set in a temperature-controlled bath and electric field strength of 3 kV/mm was applied between (+) and grounding electrode.
5. With applying electric field, silicone rubber was cured at 100°C for 1 h. After curing the sample, it was removed from the case.

Table II. Properties of $PZT_{DPZ\text{-}LQ\text{-}S1}$ and $PZT_{Z\text{-}711}$

Type	Relative permittivity	Piezoelectric strain constant d_{33} (pC/N)
$PZT_{DPZ\text{-}LQ\text{-}S1}$	4240	660
$PZT_{Z\text{-}711}$	3700	610

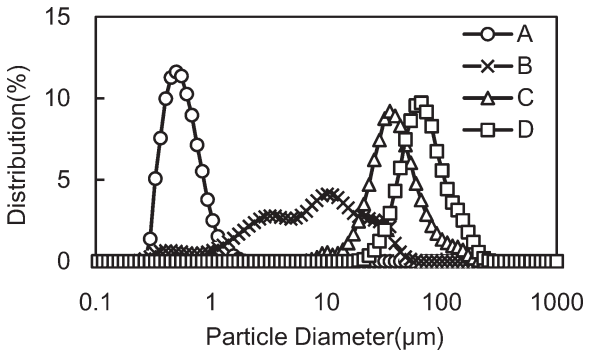

Figure 1. Particle size distribution of $PZT_{DPZ\text{-}LQ\text{-}S1}$ particles with four different particle sizes noted as A, B, C, and D.

The sample is cylindrical and the size is 50 mm in diameter and 2 mm in thickness. In addition, samples were also fabricated by applying an electric field after curing silicone rubber.

Evaluation Method of Piezoelectric Properties of Piezoelectric-Rubber

Dielectric Constant ε. In the previous investigation, the dielectric constant ε of piezoelectric-rubber increased in accordance with the enhancement of the piezoelectric properties.[17–21] It is considered that the dielectric constant ε is correlated closely with the piezoelectric properties.

Relative dielectric constant ε_r defined by dividing the dielectric constant of the samples ε by the dielectric constant of vacuum ε_0 was calculated by the following equation, after the capacitance measurement of the samples by a LCR meter at AC voltage 1 V and 1 kHz.

$$\varepsilon_r = \frac{\varepsilon}{\varepsilon_0} = \frac{C \times L}{S} / \varepsilon_0 \quad (1)$$

where C is the capacitance of the samples; L, the thickness of the samples; and S, the area of the electrode of the samples.

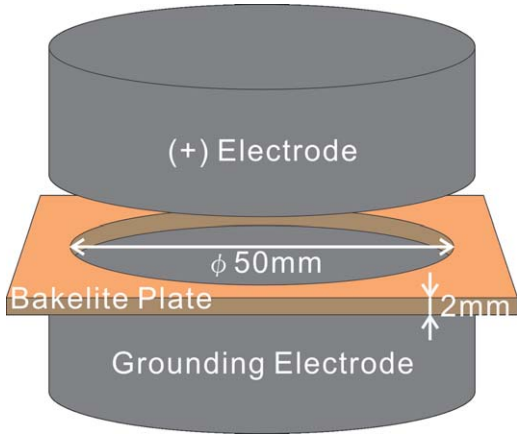

Figure 2. The case used to fabricate sample. [Color figure can be viewed in the online issue, which is available at wileyonlinelibrary.com.]

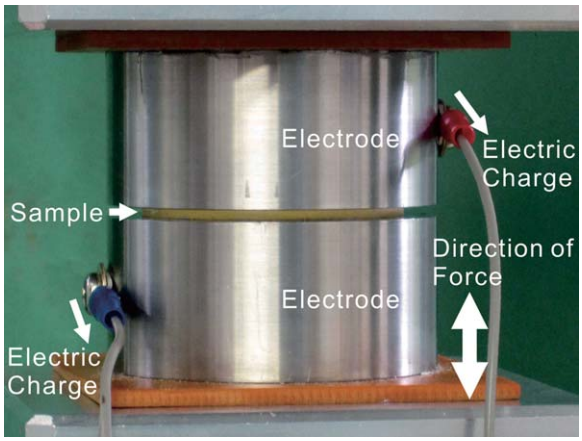

Figure 3. Photograph of the dynamic vibration test. [Color figure can be viewed in the online issue, which is available at wileyonlinelibrary.com.]

Piezoelectric Strain Constant *d*. Piezoelectric strain constant d is expressed by the following equation.

$$d = \frac{Q}{F} = \frac{\gamma}{E} \tag{2}$$

where F is the stress applied on piezoelectric materials; Q, the electric charge generated from the piezoelectric materials; E, the strength of the electric field applied to the piezoelectric materials; and γ, the strain generated from the piezoelectric materials.

The d was evaluated by dividing the amplitude value of the electric charge by the force, when a harmonic vibrating strain was applied on the sample. In this case, piezoelectric strain constant d was indicated by the following equation.

$$d = \frac{S_f Q}{S_Q F} = \frac{S_f Q_0 e^{-i\omega t}}{S_Q F_0 e^{-i\omega t}} = \frac{Q_0 S_f}{F_0 S_Q} \tag{3}$$

where S_Q was the area of electrode of the piezoelectric material; S_f, the area of applying force of the piezoelectric material; Q_0, the amplitude value of the electric charge generated from the piezoelectric material; and F_0, the amplitude value of the force. When S_f is equal to S_Q, d is Q_0/F_0.

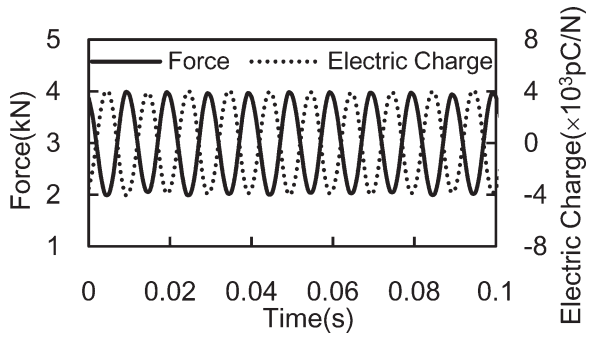

Figure 4. The time histories of the force and electric charge in dynamic vibration test for a conventional force sensor.

In this study, the harmonic vibrating strain was applied on the samples by a dynamic load machine. The sample was set between the heads of the test machine, and the harmonic vibration force was applied in the direction of thickness of the sample as shown in Figure 3.

The waveform of the vibrating force was a sine wave with the amplitude of 3 ± 1 kN at 100 Hz. After measuring the waveform of the vibrating force and generated electric charge, the amplitude value at 100 Hz of each samples were obtained by frequency analysis. The electric charge was measured by a charge amplifier. In this case, d was obtained as d_{33}, because the directions of both input force and output electric charge were vertical.

Figure 4 shows the time histories of the force and electric charge when this method is applied to a conventional force sensor using piezoelectric-ceramic supplied by FUJI CERAMIC. We observed that the charge is generated depending on the applied force, and confirmed the validity of this method because the value of d_{33} was sought calculated at -4.03 pC/N by this method as against with -4.10 pC/N, the catalog value of the sensor.

RESULTS AND DISCUSSION

Connectivity of Piezoelectric-Ceramic in Rubber

Figure 5 shows the typical connection of piezoelectric-ceramic in piezoelectric-rubber as the composite. The conventional piezoelectric-rubber was fabricated by the following method:

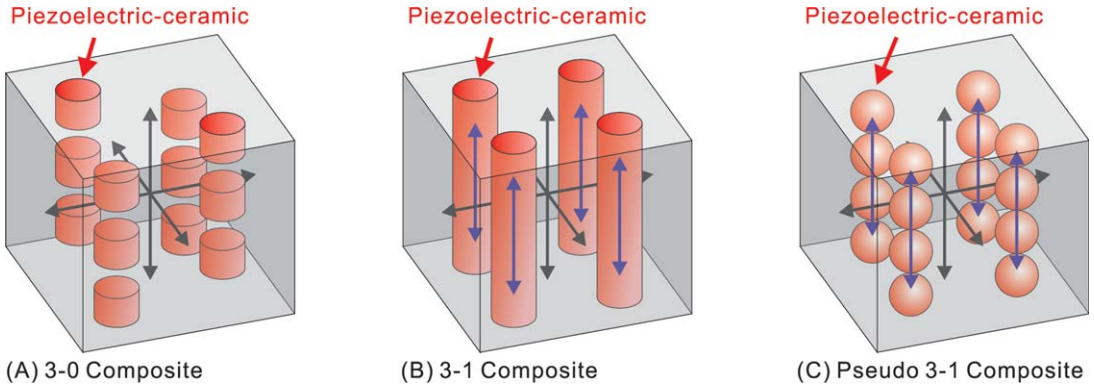

Figure 5. The typical connection of piezoelectric-ceramic in piezoelectric-rubber as the composite. [Color figure can be viewed in the online issue, which is available at wileyonlinelibrary.com.]

first, piezoelectric-ceramic particles were mixed in unvulcanized rubber and kneaded; then, the rubber was formed by vulcanization and polarized. Piezoelectric-rubber fabricated in this method forms the 3-0 composite in which the rubber is three-dimensionally vulcanized while the piezoelectric-ceramic particles are not in contact with each other [Figure 5(A)]. The piezoelectric properties of the piezoelectric-rubber of 3-0 composites were low, because the piezoelectric-ceramic particles were isolated in rubber. In the past studies, the 3-1 composite in which the rubber is three-dimensionally connected and the piezoelectric-ceramic one-dimensionally connected has more remarkable piezoelectric properties than the 3-0 composite[15–17] [Figure 5(B)]. However, in case the direction of the connection of piezoelectric-ceramic is normal to the surface, the Young's modulus of the 3-1 composite is expressed by the following equation.

$$E_c = \frac{E_p S_p + E_m S_m}{S_c} \tag{4}$$

where E_c is the Young's modulus of 3-1 composite; E_p, the Young's modulus of piezoelectric-ceramic; E_m, the Young's modulus of matrix; S_c, the area of 3-1 composite; S_p, the area of piezoelectric-ceramic; and S_m, the area of matrix.

The E_m of rubber is ~100 MPa, the E_p of piezoelectric-ceramic PZT is $\sim 10^4$ MPa. Based on the eq. (4), the Young's modulus of piezoelectric-rubber of the 3-1 composite is ~1500 MPa, in case the concentration of PZT in piezoelectric rubber is 10 vol %. As a result, the Young's modulus of the 3-1 composite of piezoelectric-rubber is dominated by piezoelectric-ceramic, and elasticity of rubber of piezoelectric-rubber is lost. It is considered that a column of piezoelectric-ceramic is formed in the direction parallel to thickness of the 3-1 composite.

Therefore, we investigated the piezoelectric-rubber of a pseudo-3-1 composite in which piezoelectric-ceramic particles were aligned normal to the rubber surface [Figure 5(C)]. In a pseudo-3-1 composite, a force applied on piezoelectric-rubber is transmitted directly to piezoelectric-ceramic particles and electric charge generated from particles was easy to conduct because these particles are connected with each other. In addition, it is considered that elasticity of piezoelectric-rubber is maintained by the following reasons. An area of contact between each particle is small and linear aggregates of particles can be inflected because piezoelectric-ceramic particles are connected by some particles in the aligned direction. As a result, the pseudo-3-1 composite has more remarkable piezoelectric properties than the 3-0 composite and more remarkable elasticity than the 3-1 composite.

Method of Forming Linear Aggregates of the Piezoelectric-Ceramic Particles

When the electric field is applied on the piezoelectric-ceramic particles, electric dipole moments of particles are induced in the direction of the electric field by polarizing them. The induced electric dipole moments vector is given by the following equation[26]

$$\mathbf{p} = 4\pi\,\varepsilon_f \varepsilon_0 \left(\frac{\varepsilon_p - \varepsilon_f}{\varepsilon_p + 2\varepsilon_f}\right) a^3 \mathbf{E} \tag{5}$$

where $\mathbf{p}$ is the electric dipole moment; $\mathbf{E}$, the electric field vector; ε_f, the dielectric constant of dielectric matrix; ε_p, the dielectric constant of piezoelectric-ceramic particles; ε_0, the dielectric constant of vacuum; and a, the radius of piezoelectric-ceramic particles.

According to the eq. (1), the induced electric dipole moments of piezoelectric-ceramic particles are influenced by the electric field intensity and the radius of piezoelectric-ceramic particles. The electric dipole moments are increased with the increase of the intensity of the electric field and radius of piezoelectric-ceramic particles.

In addition, the interacting force between two polarized piezoelectric-ceramic particles (in this case, particles denoted by i and j) placed close to each other in a dielectric material, is induced by the electric dipole moments given by the following equation[27]

$$\mathbf{F}_{ij} = \frac{3}{4\pi\varepsilon_f \varepsilon_0}\left[p^2 \frac{\mathbf{r}_{ij}}{r_{ij}^5} - 5\left(\mathbf{p}\cdot\mathbf{r}_{ij}\right)^2 \frac{\mathbf{r}_{ij}}{r_{ij}^7} + 2\left(\mathbf{p}\cdot\mathbf{r}_{ij}\right) p \frac{\mathbf{r}_{ij}}{r_{ij}^5}\right] \tag{6}$$

where $\mathbf{F}_{ij}$ is the interaction force between particles i and j; and $\mathbf{r}_{ij}$, the positional vector of i and j.

According to the eq. (6), the magnitude of interacting force on two particles in a matrix depends on the magnitude of electric dipole moments of each particle and the distance between particles. In addition, the direction in which the interaction force acts is dependent on the particle position in the electric field.

Figure 6 shows the schema of the magnitude and angle of force acting on two polarized piezoelectric-ceramic particles denoted by i and j calculated by the eq. (2). Here, it was presumed that

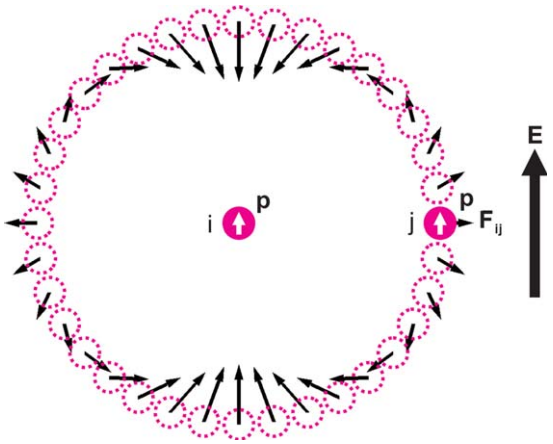

Figure 6. Schema of the magnitude and angle of forces acting on two polarized piezoelectric-ceramic particles denoted by i and j calculated by the eq. (2). [Color figure can be viewed in the online issue, which is available at wileyonlinelibrary.com.]

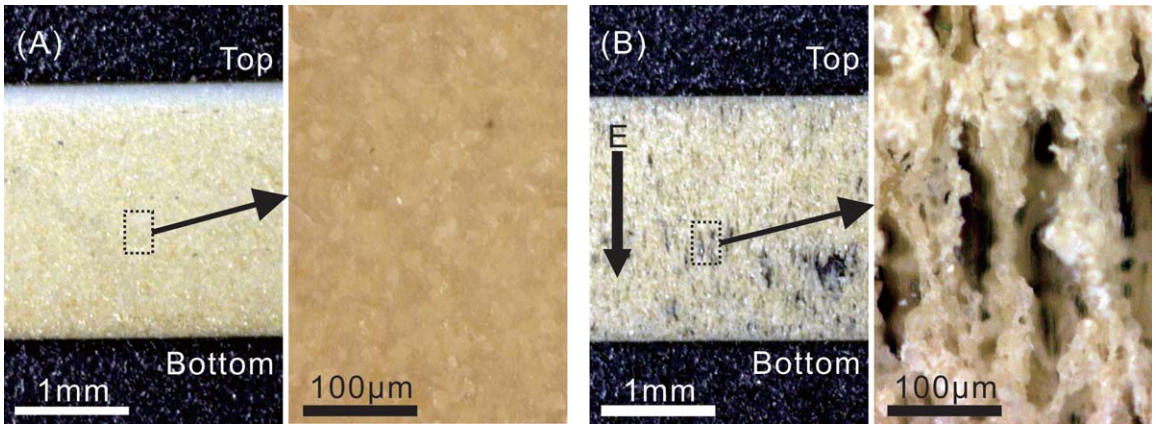

Figure 7. Photograph of the cross-sectional observation of the fabricated samples using particles C of $PZT_{DPZ\text{-}LQ\text{-}S1}$. A: Fabricated by applying electric field after curing silicone rubber. B: Fabricated by applying electric field during curing silicone rubber. [Color figure can be viewed in the online issue, which is available at wileyonlinelibrary.com.]

the position of particle *i* was fixed and the position of the particle *j* was changed along a circle. Arrow lines of the schema indicated the amount and angle of interaction force.

As a result of the calculation, the interaction force acting on two particles became maximum and they were attracted by each other, when the line connecting two particles was parallel with the electric field, and the distance between them became smaller. Moreover, when the line connecting two particles was perpendicular to the electric field, the interaction force acting between particles became smaller and kept away from each other. If many particles existed, particles, which positioned along the electric field were attracted to each other, and those that positioned perpendicular to the electric field were kept particles away from each other; after all, the piezoelectric particles were aligned and formed as linear aggregates as the pseudo-3-1 composite shown in Figure 5(C).

Observation of Fabricated Sample

Figure 7 shows the photo of the cross-sectional observation of the fabricated samples using particles C of $PZT_{DPZ\text{-}LQ\text{-}S1}$. Figure 7(A) shows the sample, which were fabricated by applying an electric field after curing silicone rubber. Figure 7(B) shows the samples were fabricated by applying an electric field during curing silicone rubber. White parts in the Figure 7 indicated $PZT_{DPZ\text{-}LQ\text{-}S1}$ particles. The concentration of PZT particles of the both samples was ~20 vol %.

The samples, which were fabricated by applying an electric field after curing silicone rubber, the large particles were settled at the bottom and the small particles ware dispersed throughout the sample. However, the samples, which were fabricated by applying an electric field during curing silicone rubber, particles were aligned and formed linear aggregates between the top end and the bottom end in the direction of the electric field. In this article, the samples, which were fabricated by an applying electric field during curing silicone rubber is referred to as the "aligned-type" and the samples, which were fabricated by an applying electric field after curing silicone rubber is referred to as the "unaligned-type." From the cross-section observation of other samples, small-sized $PZT_{DPZ\text{-}LQ\text{-}S1}$ particles in unaligned-type were dispersed randomly and large-sized ones were settled down. However, in the case of aligned-type with more than 15 vol % of concentration of $PZT_{DPZ\text{-}LQ\text{-}S1}$ particles, particles were aligned as shown in Figure 7(B); however that with <15 vol %, $PZT_{DPZ\text{-}LQ\text{-}S1}$ particles were concentrated at the top and the bottom of the sample without alignment as shown in Figure 8. Figure 8(A,B) show the sample the concentration of $PZT_{DPZ\text{-}LQ\text{-}S1}$ of which is 3 and 10 vol %, respectively. As for the cause of this phenomenon, we assumed the influence of the particle size and the particle distance depending on the particle concentration. In case the particles size is small and concentration is low, the interactive force acting on each particle is small because the induced dipole moment is small as calculated in eq. (5), and particle distance is long. As a result, particles existing nearly are aggregated near the both electrodes by coupling each particle.

Figure 9 shows a photo of observation of the aligned-type and unaligned-type using $PZT_{Z\text{-}711}$ particles; Figure 9(A), unaligned-

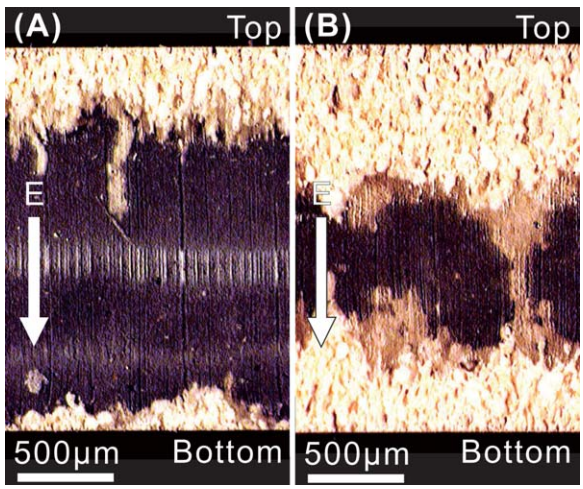

Figure 8. Photograph of the cross-sectional observation of aligned-type of low concentration particles C of $PZT_{DPZ\text{-}LQ\text{-}S1}$. A: Concentration of particle is ~3 vol %. B: Concentration of particle is ~10 vol %. [Color figure can be viewed in the online issue, which is available at wileyonlinelibrary.com.]

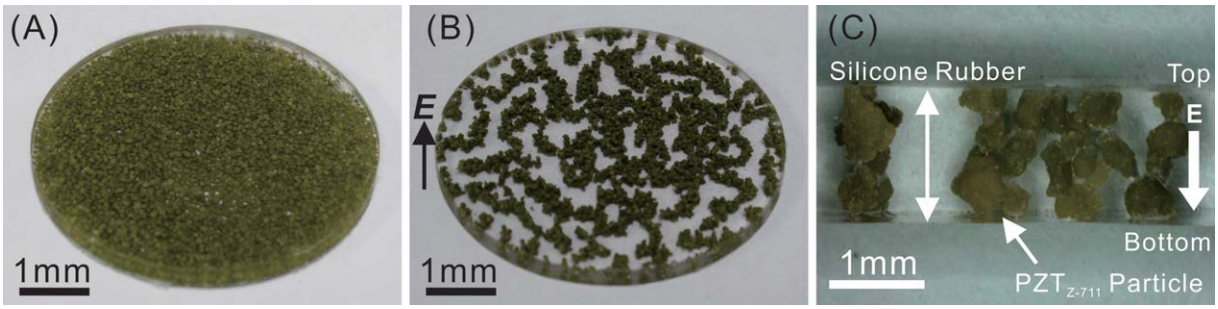

Figure 9. Photograph of observation of the aligned-type and unaligned-type using $PZT_{Z\text{-}711}$ particles; Figure 9 (A), unaligned-type; Figure 9(B), aligned-type; and Figure 9(C), cross-section observation of aligned-type. [Color figure can be viewed in the online issue, which is available at wileyonlinelibrary.com.]

type; Figure 9(B), aligned-type; and Figure 9(C), cross-section observation of aligned-type. While particles of aligned-type were aligned and formed linear aggregates between the top end and the bottom end of electrode in the direction of thickness, particles of unaligned-type were settled down on the whole area of the bottom. According to the cross-section observation of other samples, while particles of unaligned-type were settled down on the bottom at every concentration, particles of aligned-type were aligned and formed linear aggregates between the top end and the bottom end in the direction of the electric field at every concentration. Unlike the case of using particles C of $PZT_{DPZ\text{-}LQ\text{-}S1}$, $PZT_{Z\text{-}711}$ particles of aligned-type are aligned even at 10 vol % concentrations. It is considered that the interactive force acting on the particles is large because of the large size of the particles.

Effect of the Formation of Linear Aggregates and the Concentration of Particles on the ε_r

Figure 10 shows the relationship between ε_r and the concentration of $PZT_{DPZ\text{-}LQ\text{-}S1}$ particles C of both the aligned-types and unaligned-type. The dot-line of Figure 10 is the result of calculation obtained from the following Maxwell-Garnett equation.[28]

$$\varepsilon_c = \varepsilon_m \frac{\varepsilon_P + 2\varepsilon_m + 2\phi(\varepsilon_P - \varepsilon_m)}{\varepsilon_P + 2\varepsilon_m - \phi(\varepsilon_P - \varepsilon_m)} \quad (7)$$

where ε_c is the relative dielectric constant of piezoelectric-rubber; ε_m, the relative dielectric constant of silicone rubber; ε_m, the relative dielectric constant of $PZT_{DPZ\text{-}LQ\text{-}S1}$ particle; and ϕ, the volume of fraction of $PZT_{DPZ\text{-}LQ\text{-}S1}$ particle.

As the Maxwell-Garnett equation assumes that each particle is out of contact with each other and dispersed, ε_r of unaligned-type shows good agreement with the calculation result at a low concentration, although ε_r deviates a little from the calculation result at a high concentration. This result indicates that $PZT_{DPZ\text{-}LQ\text{-}S1}$ particles is out of contact with each other and dispersed at a low concentration, and the amount of particles in contact with each other increases with the increase of particle concentration. However, ε_r of aligned-type is larger than ε_r of unaligned-type and the calculation result in the range of more than 15 vol % concentrations. It is considered that increase of ε_r of aligned-type is attributable to the connection between both of electrodes by $PZT_{DPZ\text{-}LQ\text{-}S1}$ particles, which has high ε_r.

Effect of the Formation of Linear Aggregates and the Concentration of Particles on the *d*

Figure 11 shows the relationship between the concentration of $PZT_{DPZ\text{-}LQ\text{-}S1}$ C particles and d_{33} of both the aligned-types and unaligned-type. d_{33} of the aligned-type surpassed that of the unaligned-type in the concentration range of more than 15 vol %. This result was similar to the tendency of ε_r shown in Figure 10. The increase of d_{33} of aligned-type was mainly derived from the formation of linear aggregates of $PZT_{DPZ\text{-}LQ\text{-}S1}$ particles, which means that the aligned-type became similar to the pseudo-3-1 composite.

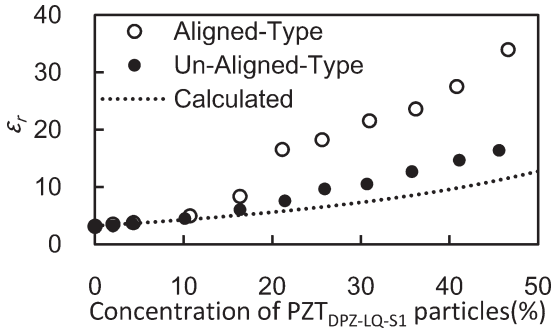

Figure 10. Relationship between ε_r and the concentration of $PZT_{DPZ\text{-}LQ\text{-}S1}$ particles C of both the aligned-types and unaligned-Type. The dot-line is the result of calculation obtained from the Maxwell-Garnett equation.

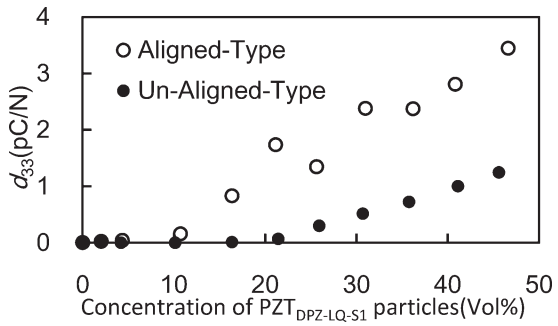

Figure 11. Relationship between the concentration of $PZT_{DPZ\text{-}LQ\text{-}S1}$ C particles and d_{33} of both the aligned-types and unaligned-type.

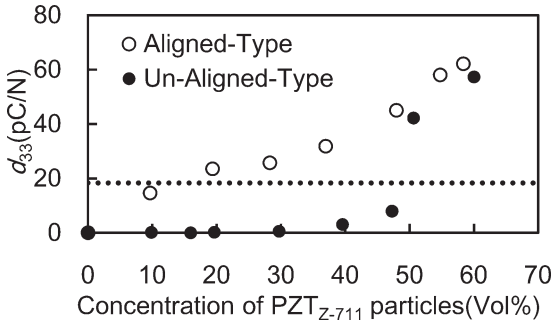

Figure 12. Relationship between the concentration of PZT_{Z-711} particles and d_{33} of both the aligned-types and unaligned-type.

Figure 12 shows the relationship between the concentration of PZT_{Z-711} particles and d_{33} of both the aligned-types and unaligned-type. The dot-line of Figure 12 is d_{33} of conventional piezoelectric-rubber mixed with PZT_{Z-711} particles of concentration 80 vol % in Chloroprene rubber.

d_{33} of the aligned-type surpassed that of the unaligned-type in the whole concentration range. And, d_{33} of aligned-type using PZT_{Z-711} particles is larger than d_{33} of aligned-type using $PZT_{DPZ-LQ-S1}$ particles. The cause of this phenomenon should be discussed in the following section. As a result of the comparison between d_{33} of conventional piezoelectric-rubber and aligned-type, aligned-type got the same d_{33} as that of the conventional piezoelectric-rubber at less than 1/4 of the concentration of PZT_{Z-711} particles in the conventional piezoelectric-rubber. This result of d_{33} indicated that PZT particle formation of linear aggregates is effective in increasing piezoelectric properties of piezoelectric-rubber.

However, d_{33} of unaligned-type sharply increased at a concentration of >50 vol % and the difference between d_{33} of aligned-type and unaligned-type became smaller in the concentration range of >50 vol %. It was considered that effect of particle alignment is reduced because movement of PZT_{Z-711} particles of aligned-type is restricted due to the increase of the amount of particles at a concentration of >50 vol %. However, Young's modulus of aligned-type at a concentration of 50 vol % is higher by more than double than Young's modulus of aligned-type at a concentration of 20 vol %. Since the purpose of this investigation is to enhance piezoelectric properties of piezoelectric-rubber by fewer piezoelectric-ceramic particles to keep rubber elasticity, we do not aim to enhance piezoelectric properties of piezoelectric-rubber at this level of concentration.

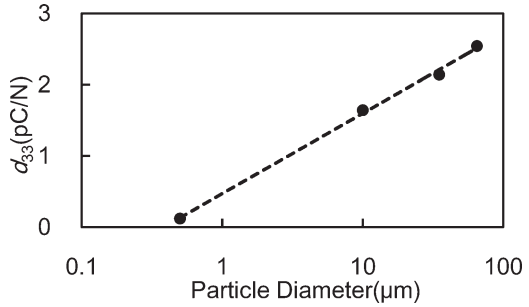

Figure 13. Relationship between d_{33} and the $PZT_{DPZ-LQ-S1}$ particles size of aligned-type.

Effect of the Particle Size on the *d*

Figure 13 shows the relationship between d_{33} and the $PZT_{DPZ-LQ-S1}$ particles size of aligned-type. In Figure 13, d_{33} is plotted against the mean diameter of particle A–D shown in Figure 1. In addition, aligned-type were prepared by mixing particles A–D, respectively, at the same concentration of ~30 vol %.

As shown in Figure 11, it was revealed that d_{33} of the aligned-types increased as the particle size increased. The reasons for the above-mentioned result are as follows.

- In the case of using larger particles, connectivity of each particle is strong by the larger induced dipole moment as show in eq. (5), and the number of particles forming linear aggregates is small. Therefore, force applied on aligned-type is transmitted more directly to PZT particles due to decrease of defection in the linear aggregates and flexion of linear aggregates.
- Due to strong connectivity of particles and decrease of defection in the linear aggregates, conducting electric charge became easier.

It is considered that the reason that d_{33} of aligned-type using PZT_{Z-711} particles greatly surpasses the d_{33} of aligned-type using $PZT_{DPZ-LQ-S1}$ particles is that PZT_{Z-711} particle size is 10 times larger than that of particle D, which is the largest of four kinds of $PZT_{DPZ-LQ-S1}$ particles.

CONCLUSIONS

Flexible piezoelectric material as a piezoelectric-rubber is expected to be used at places where the piezoelectric ceramic cannot be applied. In this investigation, the method for increasing piezoelectric properties of piezoelectric-rubber is studied. The following results were obtained.

1. A method of fabricating piezoelectric-rubber a pseudo-3-1 composite in which piezoelectric-ceramic properties is aligned in rubber is studied because piezoelectric properties of 3-1 composite is more remarkable than those of 3-0 composite. The fabrication method of "aligned-type" in which piezoelectric-ceramic particles are aligned in rubber by applying an electric field to uncured rubber mixed with piezoelectric-ceramic was suggested.
2. By the cross-section observation of aligned-type consisting of PZT particles and thermosetting silicon rubber, PZT particles forming linear aggregates parallel to the electric field was confirmed.
3. Aligned-type showed larger dielectric constant ε and piezoelectric strain constant *d* than those of piezoelectric-rubber with randomly dispersed PZT particles "unaligned-type." This result indicated that particle formation of linear aggregates is effective in increasing piezoelectric-properties of piezoelectric-rubber.
4. *d* of aligned-type increased with the increase of the concentration and the size of PZT particles.

5. The piezoelectric properties of aligned-type using PZT_{Z-711} particles of a large size were almost equal to those of conventional piezoelectric-rubber at <1/4 of the concentration of PZT particles in the conventional piezoelectric-rubber.

Piezoelectric-rubber with enhanced piezoelectric properties is expected to be used as an actuator and a sensor at places where the piezoelectric-ceramic cannot be applied. In addition, aligned-type is expected to be used as sensors for detecting faults of vibrating machines as well as material for reducing and dumping vibrations making the most of its rubber elasticity.

REFERENCES

1. Robert, L. *Appl. Opt.* **1979**, *18*, 690.
2. Hagood, N. W.; von Flotow, A. *J. Sound Vib.* **1991**, *146*, 243.
3. Date, M.; Kutani, M.; Sakai, S. J. *Appl. Phys.* **2000**, *87*, 863.
4. Yamada, K.; Mathuhisa, H.; Utsuno, H. *Jpn. Soc. Mech. Eng.* **2007**, *73*, 19.
5. Richards, C. D.; Anderson, M. J.; Bahr, D. F.; Richards, R. F. *J. Micromech. Microeng.* **2004**, *14*, 717.
6. Shu, Y. C.; Lien, I. C. *J. Micromech. Microeng.* **2006**, *16*, 2429.
7. Schröck, J.; Meuer, T.; Kugi, A. *Smart Mater. Struct.* **2011**, *20*, 1.
8. Qi, Y.; MacAlpine, M. C. *Energy Environ. Sci.* **2010**, *3*, 1275.
9. Qi, Y.; Jafferis, N. T.; Lyons, K. Jr.; Lee, C. M.; Ahmad, H.; McAlpine, M. C. *Nano. Lett.* **2010**, *10*, 524.
10. Qi, Y.; Kim, J.; Nguyen, T. D.; Lisko, B.; Purohit, P. K.; MacAlpine, M. C. *Nano Lett.* **2011**, *11*, 1331.
11. Chen, C.; Liu, J.; Jiang, X.; Luo, Y.; Yuan, F.-G.; Han, X.; Liao, J. *Proc. of SPIE* **2011**, 7983.
12. Yi, C.-H.; Lin, C.-H.; Wang, Y.-H.; Cheng, S.-Y.; Chang, H.-Y. *Ferroelecterics* **2012**, *434*, 91.
13. Newnham, R. E.; Skinner, D. P.; Cross, L. E. *Mater. Res. Bull.* **1978**, *2*, 93.
14. Skinner, D. P.; Newnham, R. E.; Cross, L. E. *Mater. Res. Bull.* **1978**, *13*, 599.
15. Newnham, R. E.; Bowen, L. J.; Klicker, K. A.; Cross, L. E. *Mater. Eng.* **1980**, *2*, 93.
16. Klicker, K. A.; Biggers, J. V.; Newnham, R. E. *J. Am. Ceram. Soc.* **1982**, *64*, 5.
17. Banno, H.; Saito, S. *Jpn. J. Appl. Phys.* **1983**, *22*, 67.
18. Banno, H. *Ferroelectrics* **1983**, *50*, 3.
19. Safari, A.; Halliyal, A.; Bowen, L. J.; Newnham, R. E. *J. Am. Ceram. Soc.* **1982**, *65*, 207.
20. Newnham, R. E.; Safari, A.; Sa-gong, G.; Giniewicz, J. *Proc. IEEE Ultrasonic Symp.* **1984**, *1*, 501.
21. Mamada, S.; Yaguti, N.; Suzuki, M.; Hansaka, M. *Koubunshi Ronbunshu* **2008**, *65*, 579.
22. Winslow, W. M. *J. Appl. Phys.* **1949**, *20*, 1137.
23. Klingenberg, D. J.; van Swol, F.; Zukoski, C. F. *J. Chem. Phys.* **1989**, *91*, 7888.
24. Klingenberg, D. J.; Zukoski, C. F. *IV. Langmuir* **1990**, *6*, 15.
25. Shiga, T.; Okada, A.; Kurauchi, T. *Macromolecules*, **1993**, *26*, 6958.
26. Morishita, S.; Shiraishi, T. *Dyn. Des. Conf.* **1998**, *98*, 299.
27. Yamamoto, S. *R&D Rev. Toyota CRDL* **1994**, *29*, 39.
28. Kärkkäine, K. K.; Sihvola, A. H.; Nikoskinen, K. I. *IEEE Trans. Geosci. Remote Sens.* **2001**, *39*, 1013.